This is a preprint of a paper published in *J. Am Chem. Soc.* **2008**, *130*, 6362-6366.

Encapsulation of Protonated Diamines in a Water-Soluble Chiral, Supramolecular Assembly Allows for Measurement of Hydrogen-Bond Breaking Followed by Nitrogen Inversion/Rotation (NIR)[1]

Michael D. Pluth, Robert G. Bergman, and Kenneth N. Raymond**

Contribution from the Department of Chemistry, University of California, and Chemistry Division, Lawrence Berkeley National Laboratory, Berkeley, California, 94720, USA

Corresponding Authors:

Prof. Robert G. Bergman, Prof. Kenneth N. Raymond, Department of Chemistry, University of California, Berkeley, CA 94720-1460 (USA). Fax: (+1) 510-642-7714 (Bergman). Fax: (+1) 510-486-5283 (Raymond). E-mail: rbergman@berkeley.edu, raymond@socrates.berkeley.edu

Abstract Amine nitrogen inversion, difficult to observe in aqueous solution, is followed in a chiral, supramolecular host molecule with purely-rotational *T*-symmetry that reduces the local symmetry of encapsulated monoprotonated diamines and enables the observation and quantification of $\Delta G^{\ddagger}$ for the combined hydrogen-bond breaking and nitrogen inversion rotation (NIR) process. Free energies of activation for the combined hydrogen-bond breaking and NIR process inside of the chiral assembly were determined by the NMR coalescence method. Activation parameters for ejection of the protonated amines from the assembly confirm that the NIR process responsible for the coalescence behavior occurs inside of the assembly rather than by a guest ejection / NIR / re-encapsulation mechanism. For one of the diamines, *N,N,N′,N′*-tetramethylethylenediamine (TMEDA), the relative energy barriers for the hydrogen-bond breaking and NIR process were calculated at the G3(MP2)//B3LYP/6-31++G(d,p) level of theory, and these agreed well with the experimental data.

Introduction

Nitrogen pyramidal inversion (umbrella inversion motion) in amines involves moving the lone pair from one side of the tetrahedral amine structure to the other. Studies of amine nitrogen inversion have come from most disciplines of chemistry including theoretical, computational, synthetic and biological.[2-6] However, direct measurement of the rapid rate of this transformation in solution is difficult. Most measurements of the inversion free energy barrier[7] have come from gas-phase far-infrared or microwave spectroscopies.[8] Inversion barriers in the gas phase for alkylamines generally do not exceed 9 kcal/mol but steric hindrance, hybridization changes or hydrogen bonding can increase the barrier by $\geq$ 5 kcal/mol.[9] Most measurements of nitrogen inversion barriers in solution have come from NMR solution studies and rely on monitoring changes in the chemical environment of functional groups near the nitrogen atom. This can be aided by monitoring enantiotopic hydrogens to the nitrogen of prochiral amines or monitoring the NMR spectra of prochiral amines as a function of pH. [9-13] Although often referred to as nitrogen inversion in the literature, solution measurements of the

inversion process almost always measure a combined nitrogen-inversion rotation (NIR) which is required to change the chemical environment of the functional groups being monitored.[14, 15]

Due to the experimental difficulties of probing NIR processes with low activation barriers by NMR, most NMR studies have necessarily focused on amines with higher inversion barriers enforced by specific structural or electronic constraints, such as those in aziridines (10-20 kcal/mol),[16, 17] diaziridines (20 – 30 kcal/mol),[18, 19] azanorbornanes (>13 kcal/mol),[20, 21] hydrogen-bonded amines (10 – 20 kcal/mol).[9, 22] or sterically hindered amines.[14] Recent work has also focused on controlling the rate of nitrogen inversion by a variety of strategies, such as redox switching[23] or metal coordination.[24] Herein, we report the use of the constrained guest environment of a self-assembled supramolecular assembly to detect the NIR of encapsulated monoprotonated diamines and to quantify the associated energy barriers for the process.

Results and Discussion

We have previously described the formation and chemistry of the tetrahedral supramolecular assembly $[Ga_4L_6]^{12-}$ (L = *N,N*′-bis(2,3-dihydroxybenzoyl)-1,5-diaminonaphthalene) (**1**) (Figure 1).[25-28] The −12 overall charge of **1** imparts water solubility, while the naphthalene walls provide a hydrophobic cavity which is isolated from the bulk aqueous solution. The tris-bidentate coordination at the metal vertices makes each vertex a stereocenter and the strong mechanical coupling of the ligands transfers the chirality of one metal vertex to the others (forming the mirror image ΔΔΔΔ or ΛΛΛΛ homochiral enantiomers of the assembly).[29] With purely rotational *T* point group symmetry, **1** has been exploited for the diastereoselective encapsulation and reactivity of organometallic complexes and the dynamic resolution of ruthenium sandwich and half-sandwich complexes.[30] We have recently reported the ability of **1** to encapsulate monoprotonated amines and dramatically increase the basicity of the encapsulated guest,[31] a property that was used to facilitate the acid-catalyzed hydrolysis of encapsulated orthoformates[32] and acetals[33] in basic solution. Following the amine protonation studies, we hoped to use the chirality of **1** to observe the NIR process of encapsulated diamine guests.

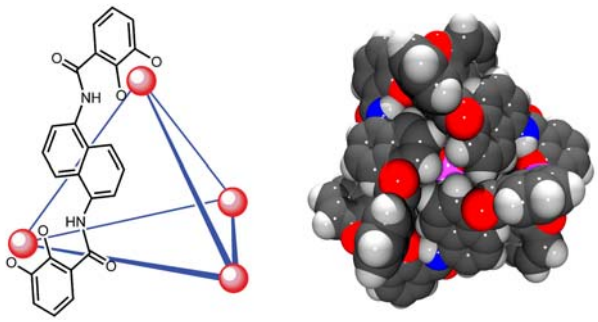

Figure 1. (Left) A schematic representation of **1** with only one ligand shown for clarity. (Right) A space-filling model of **1**.

Although chelating diamines such as *N,N,N′,N′*-tetramethylethylenediamine (**2**) have idealized C_{2v} symmetry, encapsulation in the chiral *T*-symmetric host reduces the symmetry of the guest to C_2. This renders the geminal nitrogen methyl groups inequivalent, which enables detection of hydrogen-bond breaking followed by NIR by ^{1}H NMR. One possible mechanism for the NIR for chelating amines is outlined in Scheme 1. In the initial structures, the "A" (blue) and "B" (red) methyl groups are inequivalent due to the symmetry imposed by **1**. Breaking one N-H hydrogen bond (a) allows one nitrogen stereocenter to invert (b) followed next by bond rotation (c) and finally by reformation of the hydrogen bond (d).[34] In this process the "A" and "B" methyl groups exchange. If this process occurs rapidly on the NMR time scale, only one resonance corresponding to the methyl groups will be observed. Conversely, if the exchange process is slow on the NMR time scale, two methyl resonances should be observed. Furthermore, the constrained environment of the interior cavity of **1** should increase the inversion barrier of encapsulated protonated amines thereby facilitating detection.

Scheme 1.

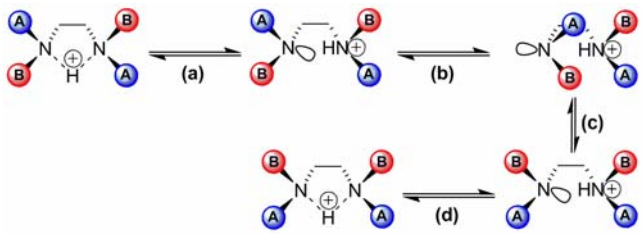

In screening potential guests, a number of monoamines and diamines containing geminal *N*-alkyl groups were investigated. Our recent work with protonated amine and phosphine guests has shown that the guests are encapsulated in their monoprotonated form.[31] The host-guest complexes of the encapsulated protonated amines in **1** are stable in both aqueous and non-aqueous solutions. Neutral guests can also be encapsulated in **1**, but since the encapsulation is driven by the hydrophobic effect, addition of non-aqueous solvents prohibits encapsulation.[35]

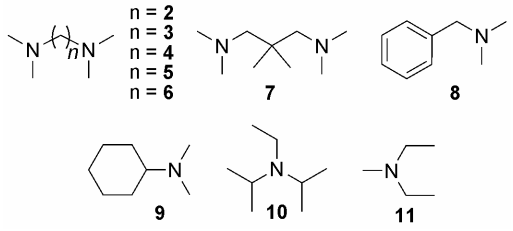

Figure 2. Scope of monoamines and diamines investigated

At room temperature in D_2O, the ^1H NMR of host-guest complexes of amines such as **2** and **3** showed only one signal corresponding to the geminal *N*-methyl groups on the nitrogens, suggesting fast NIR on the NMR timescale. However, in the case of **4**, two distinct geminal methyl signals were observed, suggesting that the hydrogen-bond breaking / NIR process was slow on the NMR timescale. The freezing point of water limited accessible temperatures low enough to observe decoalesence of the averaged resonances for amines **2** and **3**. Therefore, methanol was used as a solvent to obtain a greater temperature range for variable temperature experiments. This solvent choice was also advantageous since it prevents encapsulation of the neutral form of the guests. Lowering the temperature of an amine-

encapsulated complex in methanol did slow the hydrogen-bond breaking / NIR process sufficiently, such that decoalescence in the ^{1}H NMR spectrum was observed. As the temperature was lowered, the peak corresponding to the *N*-alkyl protons broadened and then separated into two different resonances (Figure 3).

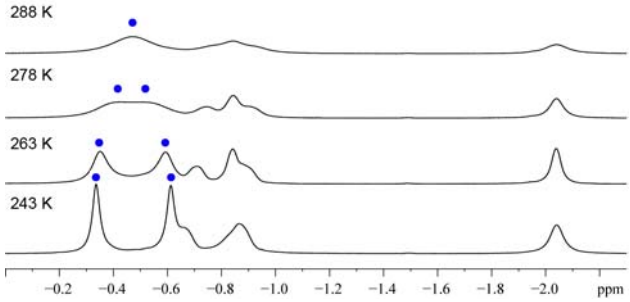

Figure 3. Variable temperature ^{1}H NMR spectra of encapsulated *N,N,N′,N′*-tetramethyl-1,5-diaminopentane (**5**). Methyl resonances are highlighted with blue (▯) (500 MHz, CD_3OD, 15 mM **1**)

By monitoring each host-guest complex as a function of temperature, coalescence behavior was observed for the geminal *N*-alkyl groups on amines **2-11**. Measurement of the difference in Hertz (Δ▯) between the decoalesced peaks at the slow exchange limit allows for the determination of the rate of exchange at the point of coalescence (eq. 1). By determining the coalescence temperature (T_c) for the hydrogen-bond breaking / NIR process, the free energy of activation for the coalescence process can be determined by standard methods (eq. 2).[36,37]

$$k_c = \frac{\pi}{\sqrt{2}}\left|\Delta\upsilon\right| \qquad (1)$$

$$\Delta G^{\ddagger} = R \cdot T_c \cdot \ln\left(\frac{R \cdot T_c}{k_c \cdot N_A \cdot h}\right) \qquad (2)$$

Based on the mechanism for hydrogen-bond breaking followed by NIR described in Scheme 1, it was somewhat unexpected that monoamines showed coalescence behavior, since the proposed mechanism requires a second nitrogen atom to bind the proton as the other nitrogen inverts. An alternative mechanism for the observed NMR coalescence could involve guest exchange, in which an encapsulated amine is ejected from **1**, inverts (or undergoes NIR) in free solution, and is then re-encapsulated. This would require that the inversion barrier in solution be lower than in **1**, consistent with the highly sterically crowded interior of **1**. A qualitative energy diagram for amine encapsulation followed by hydrogen-bond breaking and NIR is shown in Figure 4. If the activation barrier for guest exchange ($\Delta G^{\ddagger}_{exch}$) is larger than the activation barrier for hydrogen-bond breaking and NIR ($\Delta G^{\ddagger}_{NIR}$), the NIR will occur faster than guest exchange and be observed in the assembly. However, if $\Delta G^{\ddagger}_{NIR}$ is equal to or greater than $\Delta G^{\ddagger}_{exch}$, then the observed $\Delta G^{\ddagger}_{NIR}$ should be equal to $\Delta G^{\ddagger}_{exch}$, meaning that the coalescence behavior is due to guest exchange rather than the hydrogen-bond breaking and NIR process. Due to the fact that the geminal methyl groups are both enantiotopic and isosteric, the ground-state energy of the encapsulated amine is not changed after inversion.

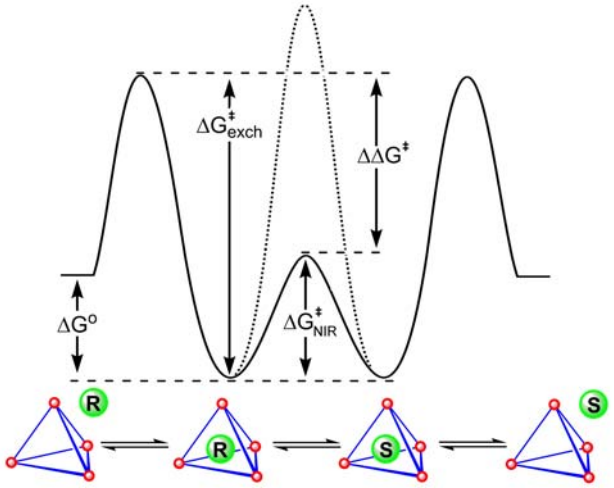

Figure 4. Energy diagram for amine exchange and inversion in **1**. Solid line: $\Delta G^{\ddagger}_{NIR} < \Delta G^{\ddagger}_{exch}$, Dotted line: $\Delta G^{\ddagger}_{exch} < \Delta G^{\ddagger}_{NIR}$. R and S refer to the two forms of the amine where the geminal *N*-methyl groups have changed places. $\Delta G^{\ddagger}_{NIR}$ refers to the combined hydrogen-bond breaking / NIR process.

In order to confirm that the NIR process responsible for the coalescence behavior was occurring inside **1** rather than free in solution, the energy barriers for guest exchange were determined using Eyring analysis of guest exchange rates measured using the selective inversion recovery NMR method at different temperatures.[38] (See Supporting Information for a complete listing of activation enthalpies and entropies $\Delta S^{\ddagger}$ and $\Delta H^{\ddagger}$ for the guest exchange process). Based on the activation parameters for guest exchange, $\Delta G^{\ddagger}_{exch}$ was calculated at the determined coalescence temperature. Comparisons of the free energy of activation barrier for guest exchange ($\Delta G^{\ddagger}_{exch}$) and the activation barrier for the coalescence process ($\Delta G^{\ddagger}_{coal}$) are shown in Table 1. For chelating amines (**2**-**7**), the barrier corresponding to the coalescence process is lower than the exchange barrier suggesting that the coalescence behavior is due to the hydrogen-bond breaking / NIR process occuring in **1**. This provides strong support for the conclusion that NIR is occurring inside the cavity of **1** (i.e. $\Delta\Delta G^{\ddagger} > 0$, Figure 3.) and shows that the hydrogen-bond breaking / NIR process happens much more quickly than guest exchange. For the small chelating diamines **2** and **3**, the difference between the inversion barrier and guest exchange is greater than 6 kcal/mol, which corresponds to the NIR process occurring ~10,000 times as often as guest exchange.

Table 1 Comparison of activation parameters for guest exchange ($\Delta G^{\ddagger}_{exch}$) and energy barriers for amine inversion inside of **1** ($\Delta G^{\ddagger}_{NIR}$).

Guest	T_c (K)	$\Delta G^{\ddagger}_{coal}$ (kcal mol^{-1})	$\Delta G^{\ddagger}_{exch}$ [a] (kcal mol^{-1})	$\Delta\Delta G^{\ddagger}$ [b] (kcal mol^{-1})
2	244 ± 2	11.0 ± 0.2	17.2 ± 0.2	6.2 ± 0.3
3	231 ± 2	10.3 ± 0.2	16.9 ± 0.8	6.6 ± 0.8
4	344 ± 2	15.7 ± 0.2	19.1 ± 0.5	3.4 ± 0.5
5	293 ± 2	13.5 ± 0.2	15.1 ± 0.2	1.6 ± 0.3
6	288 ± 2	13.1 ± 0.2	15.0 ± 0.6	1.9 ± 0.7
7	339 ± 2	16.2 ± 0.2	19.7 ± 0.8	3.5 ± 0.9
8	328 ± 2	14.2 ± 0.2	14.8 ± 0.9	0.6 ± 0.8
9	326 ± 2	14.9 ± 0.2	14.2 ± 0.3	-0.7 ± 0.3
10	347 ± 2	16.8 ± 0.2	17.5 ± 0.9	0.7 ± 0.9
11	293 ± 2	13.8 ± 0.2	13.3 ± 0.7	-0.5 ± 0.7

[a] Calculated at T_c. [b] $\Delta\Delta G^{\ddagger} = \Delta G^{\ddagger}_{exch} - \Delta G^{\ddagger}_{NIR}$

In contrast to the protonated diamines (**8**-**11**), protonated monoamines showed identical activation barriers for guest exchange and coalescence. For diamines, one nitrogen can bind the proton while the other nitrogen inverts. Monoamines, however, cannot release the proton when encapsulated in **1**. The only way the deprotonation / NIR process can occur with monamines is for the encapsulated protonated amine to be ejected from **1** where it can then undergo deprotonation followed by NIR and then re-encapsulation (Scheme 2). If this is occurring, then the free energy of activation for guest exchange and the NIR process should be equal which, as expected, is observed.

Scheme 2.

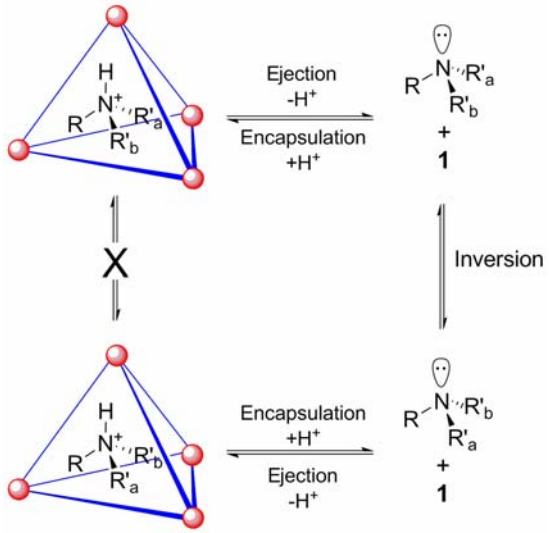

In further study of the NIR mechanism, we sought to probe the energetics of the individual steps necessary for NIR to occur. Calculations were performed in Gaussian 03 at the G3(MP2)//B3LYP/6-31++G(d,p) level of theory (Figure 6) using **2** as the model substrate. The first energetic barrier investigated was the proton transfer between the two nitrogens, which proceeds through the symmetric structure in **TS1**. As expected, the barrier for proton transfer is low $\Delta H^{\ddagger}$ = 2.4 kcal/mol (Figure 6A).

The NIR process detected by variable temperature ^{1}H NMR studies could occur by one of two pathways, one requiring nitrogen inversion and rotation around the C-N bond, and the other requiring nitrogen inversion and rotation around both the C-C and C-N bonds (Figure 6). It may appear as if the transformations described in Figure 6 violate the Principle of Microscopic Reversibility; however, it

should be noted that the conversions start and end at the same point on the potential energy surface. This makes the reaction coordinates cyclic in nature and generates the required symmetry of the reaction coordinate. In the first pathway, the nitrogen inverts directly from the ground state structure **2** through **TS2** ($\Delta H^{\ddagger}$ = 11.3 kcal/mol) to lead to intermediate **12**. Rate limiting rotation around the C-N bond (**TS3**, $\Delta H^{\ddagger}$ = 16.3 kcal/mol) then occurs to lead to back to **1**, in which the two geminal methyl groups on the inverting nitrogen have changed places.

The second pathway, which includes both C-C and C-N bond rotation, begins with breaking of the hydrogen bond between the nitrogen and protonated amine followed by rotation around the C-C bond (**TS4**, $\Delta H^{\ddagger}$ = 10.3 kcal/mol) leading to **13** where the proton is no longer chelated. Inversion of the nitrogen (**TS5**, $\Delta H^{\ddagger}$ = 15.8 kcal/mol) leads to the inverted intermediate **14**. Subsequent C-C bond rotation (**TS6**, $\Delta H^{\ddagger}$ = 2.4 kcal/mol) leads back to **12** which then undergoes C-N bond rotation in the same manner as in pathway (b) (**TS3**, $\Delta H^{\ddagger}$ = 16.3 kcal/mol).

All of the steps in paths (b) and (c) are completely reversible and proceed through the same rate-limiting step (**TS3**) so are likely all contributing to the observed coalescence behavior. For the encapsulated species, pathway (b) may be more prevalent since it leads through a more compact transition state than structures generated from C-C bond rotation in pathway (c). The longest linear dimension for the structures in pathway (c) where the proton is not chelated is greater than the more compact structures in pathway (b) suggesting that upon encapsulation in **1**, steric interactions with the naphthalene walls of **1** may play an important role in selecting which of the two pathways is most active.

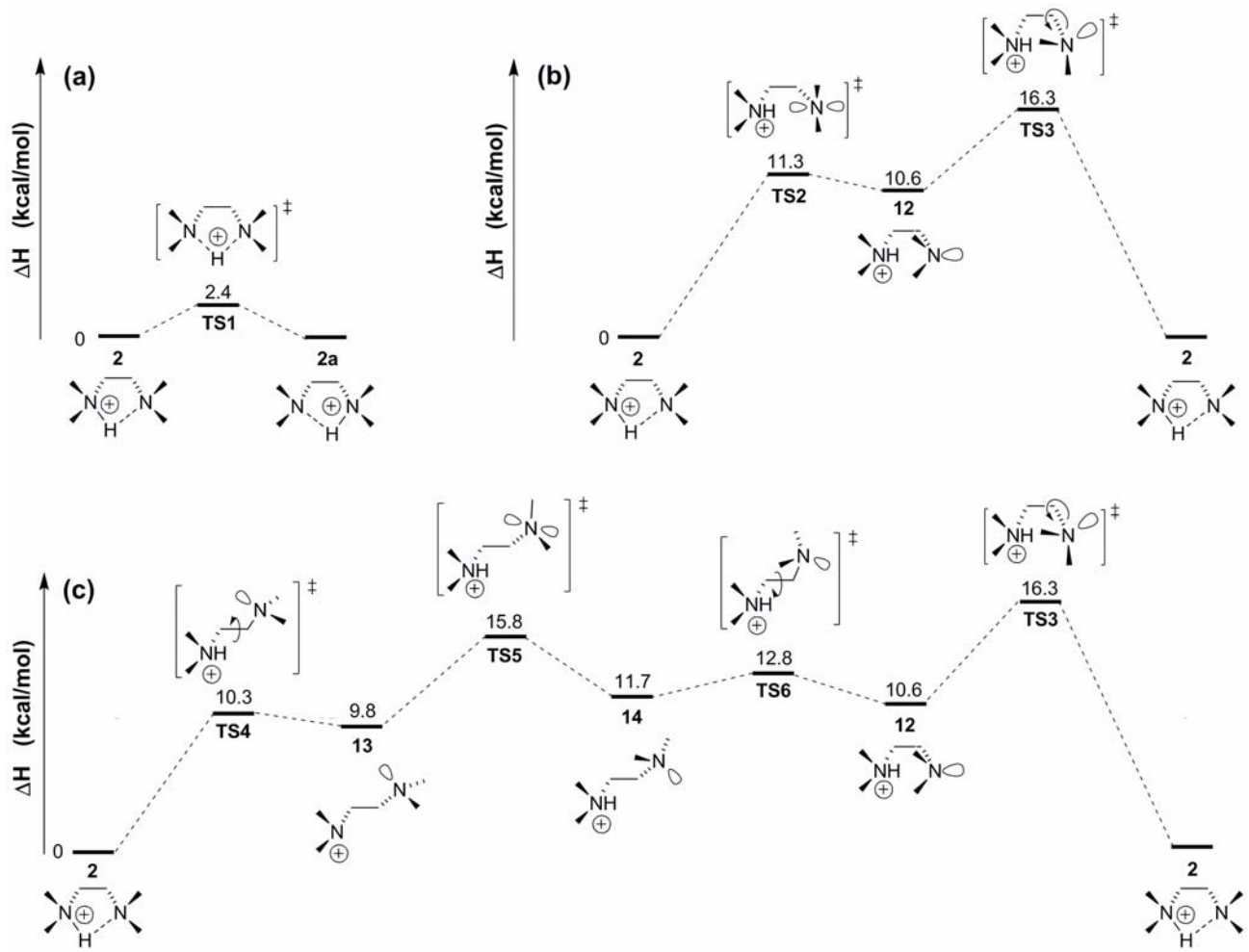

Figure 5. Calculated (G3(MP2)//B3LYP/6-31++G(d,p)) energy coordinate diagram for (a) proton transfer, (b) NIR without C-C bond rotation, and (c) NIR with C-C bond rotation.

Conclusion

The study of nitrogen inversion is a classic problem in chemistry and is usually is not observable in solution. However, exploiting the confined and chiral cavity of a synthetic host molecule enables this observation for protonated diamine guests in water. The strategy of using local symmetry reduction can potentially be used as a powerful tool to study a wide variety of important chemical phenomena that would otherwise be difficult or otherwise impossible to observe.

Experimental Section

General Procedures All NMR spectra were obtained using a Bruker AV-500 MHz spectrometer. The temperature of all variable temperature NMR experiments was calibrated with methanol or ethylene

glycol standards.[39] Selective Inversion Recovery (SIR)[38, 40, 41] experiments were performed at constant temperature using a 10 second delay time between experiments. Data points for each Selective Inversion Recovery experiment were measured using one scan with a pre-scan delay of ten seconds. Mixing times were varied from 0.0005 seconds to 18 seconds in 42 increments. In all cases, the efficiency of the inversion pulse was greater than 70%.

Computational Methods All calculations were performed using the Gaussian 03 software package with the GaussView graphical user interface.[42] Geometry optimizations, transition state searches, and unscaled frequency calculations were carried out at the B3LYP/6-31G++(d,p) level of theory. Frequency calculations were performed on all converged structures to confirm that they corresponded to local minima or transition states on their respective potential-energy surfaces. Transition states were characterized by the presence of exactly one imaginary frequency. These structures and frequencies were then used as input in the G3(MP2) zero-point corrected enthalpy calculations.[43, 44] Initial structures for transition states related to bond rotations were obtained by driving the dihedral angle around the relevant bond in five degree increments at the semiempirical (AM1) level of theory.[45]

Materials. Amines **2**-**4**, **10**, and **11** were obtained from Aldrich and used as received. Deuterated methanol was purchased from Cambridge Isotope Laboratories, and degassed by three freeze-pump-thaw cycles. Amines **5**,[46] **8**[47] and **9**[48] were prepared by reductive methylation as described in the literature. The host assembly $K_{12}[Ga_4L_6]$ was prepared as described in the literature and precipitated with acetone.[25]

General Procedure for Amine Encapsulation In an N_2-filled glovebox, 15.0 mg of $K_{12}Ga_4L_6$ were added to an NMR tube at which point 0.5 mL of CD_3OD was added. The amine (5.0 equiv.) was added by syringe and the NMR tube was shaken for 30 seconds. For amines with high coalescence temperatures, the NMR tubes were flame-sealed under vacuum. *Caution*: Heating sealed NMR tubes in an NMR probe to temperatures above the boiling point of the solvent should be done with great care.

^{1}H NMR data for the encapsulated mono-protonated amines both above and below the coalescence temperature are included in the Supporting Information.

Acknowledgment. We thank Dr. Dennis Leung for helpful discussions, Dr. Jamin Krinsky and Dr. Kathleen Durkin at the UCB Molecular Graphics Facility (NSF grant CHE-0233882) for assistance with calculations, and Dr. Herman van Halbeek and Rudi Nunlist for NMR assistance. This work was supported by the Director, Office of Science, Office of Basic Energy Sciences, and the Division of Chemical Sciences, Geosciences, and Biosciences of the U.S. Department of Energy at LBNL under Contract No. DE-AC02-05CH11231and an NSF predoctoral fellowship to M.D.P.

Supporting Information Available: Experimental details, NMR characterization, Eyring plots, and further computational details including optimized geometries, calculated total energies, and calculated frequencies. This material is available free of charge via the Internet at http://pubs.acs.org.

References

(1) Paper number 40 in the series Coordination Number Incommensurate Cluster Formation. For the previous paper in the series see: Pluth, M. D.; Tiedemann, B. E. F.; van Halbeek, H.; Nunlist, R.; Raymond, K. N. *Inorg. Chem.*; **2008**; ASAP Article.

(2) Costain, C. C.; Sutherland, G. B. B. M., *J. Phys. Chem.* **1952,** 56, 321.

(3) Goux, W. J.; Teherani, J.; Sherry, A. D., *Biophys. Chem.* **1984,** 19, 363.

(4) Perrin, C. L.; Thoburn, J. D.; Elsheimer, S., *J. Org. Chem.* **1991,** 56, 7034.

(5) Andersen, J. E.; Tocher, D. A.; Casarini, D.; Lunazzi, L., *J. Org. Chem.* **1991,** 56, 1731.

(6) Schwerdtfeger, P., *J. Chem. Phys.* **1992,** 96, 6807.

(7) All of the energy barriers measured in this paper are free energies of activation.

(8) Smeyers, Y. G.; Villa, M., *Chem. Phys. Lett.* **2000,** 324, 273.

(9) Denisov, G. S.; Gindin, V. A.; Golubev, N. S.; Koltsov, A. I.; Smirnov, S. N.; Rospenk, M.; Koll, A.; Sobczyk, L., *Mag. Res. Chem.* **1993,** 31, 1034.

(10) Saunders, M.; Yamada, F., *J. Am. Chem. Soc.* **1963,** 85, 1882.

(11) Bardos, T. J.; Szantay, C.; Navada, C. K., *J. Am. Chem. Soc.* **1965,** 87, 5796.

(12) Griffith, D. L.; Roberts, J. D., *J. Am. Chem. Soc.* **1965,** 87, 4089.

(13) Morgan, W. R.; Leyden, D. E., *J. Am. Chem. Soc.* **1970,** 92, 4527.

(14) Belostotskii, A. M.; Gottlieb, H. E.; Aped, P.; Hassner, A., *Chem. Eur. J.* **1999,** 5, 449.

(15) Belostotskii, A. M.; Hassner, A., *J. Phys. Org. Chem.* **1999,** 12, 659.

(16) Drakenberg, T.; Lehn, J.-M., *J. Chem. Soc., Perkin Trans. 2* **1972**, 532.

(17) Splitter, J. S.; Calvin, M., *Tet. Lett.* **1973,** 42, 4111.

(18) Mannschreck, A.; Seitz, W., *Angew. Chem. Int. Ed.* **1969,** 8, 212.

(19) Trapp, O.; Schurig, V.; Kostyanovsky, R. G., *Chem. Eur. J.* **2004,** 10, 951.

(20) Nelson, S. F.; Ippoliti, J. T.; Frigo, T. B.; Petillo, P. A., *J. Am. Chem. Soc.* **1989,** 111, 1776.

(21) Belostotskii, A. M.; Gottlieb, H. E.; Hassner, A., *J. Am. Chem. Soc.* **1996,** 118, 7783.

(22) Belostotskii, A. M.; Gottlieb, H. E.; Aped, P., *Chem. Eur. J.* **2002,** 8, 3016.

(23) Davies, M. W.; Shipman, M.; Tucker, J. H. R.; Walsh, T. R., *J. Am. Chem. Soc.* **2006,** 128, 14260.

(24) Davies, M. W.; Clarke, A. J.; Clarkson, G. J.; Shipman, M.; Tucker, J. H. R., *Chem. Commun.* **2007**, 5078.

(25) Caulder, D. L.; Powers, R. E.; Parac, T. N.; Raymond, K. N., *Angew. Chem. Int. Ed.* **1998,** 37, 1840.

(26) Caulder, D. L.; Raymond, K. N., *J. Chem. Soc, Dalton Trans. Inorg. Chem.* **1999,** 8, 1185.

(27) Davis, A. V.; Fiedler, D.; Seeber, G.; Zahl, A.; van Eldik, R.; Raymond, K. N., *J. Am. Chem. Soc.* **2006,** 128, 1324.

(28) Davis, A. V.; Raymond, K. N., *J. Am. Chem. Soc.* **2005,** 127, 7912.

(29) Davis, A. V.; Fiedler, D.; Ziegler, M.; Terpin, A.; Raymond, K. N., *J. Am. Chem. Soc.* **2007,** 129, 15354.

(30) Fiedler, D.; Leung, D. H.; Bergman, R. G.; Raymond, K. N., *Acc. Chem. Res.* **2005,** 38, 349.

(31) Pluth, M. D.; Bergman, R. G.; Raymond, K. N., *J. Am. Chem. Soc.* **2007,** 129, 11459.

(32) Pluth, M. D.; Bergman, R. G.; Raymond, K. N., *Science* **2007,** 316, 85.

(33) Pluth, M. D.; Bergman, R. G.; Raymond, K. N., *Angew. Chem. Int. Ed.* **2007,** 46, 8587.

(34) Bond rotation could also precede nitrogen inversion.

(35) Biros, S. M.; Bergman, R. G.; Raymond, K. N., *J. Am. Chem. Soc.* **2007,** 129, 12094.

(36) Allerhand, A.; Gutowsky, H. S.; Jonas, J.; Meinzer, R. A., *J. Am. Chem. Soc.* **1966,** 88, 3185.

(37) Line-shape analysis was not possible due to peak broadening upon encapsulation.

(38) Bain, A. D.; Cramer, J. A., *J. Magn. Reson. A* **1996,** 118, 21.

(39) Amman, C.; Meier, P.; Merbach, A. E., *J. Magn. Reson. A* **1982,** 46, 319.

(40) Perrin, C. L.; Dwyer, T. J., *Chem. Rev.* **1990,** 90, 935.

(41) Bain, A.; Cramer, J. A., *J. Magn. Reson. A* **1993,** 103, 217.

(42) Frisch, M. J., et al. *Gaussian 03, Revision D.01*, Gaussian, Inc.: Wallingford CT, 2004.

(43) Curtiss, L. A.; Redfern, P. C.; Raghavachari, K.; Rassolov, V.; Pople, J. A., *J. Chem. Phys.* **1999,** 110, 4703.

(44) Baboul, A. G.; Curtiss, L. A.; Redfern, P. C.; Raghavachari, K., *J. Chem. Phys.* **1999,** 110, 7650.

(45) Dewar, M.; Thiel, W., *J. Am. Chem. Soc.* **1977,** 99, 2338.

(46) Halpern, A. M.; Legenza, M. W.; Ramachandran, B. R., *J. Am. Chem. Soc.* **1979,** 101, 5736.

(47) Clarke, H. T.; Gillespie, H. B.; Weisshaus, S. Z., *J. Am. Chem. Soc.* **1933,** 55, 4571.

(48) Cope, A. C.; LeBel, N. A.; Lee, H. H.; Moore, W. R., *J. Am. Chem. Soc.* **1957,** 79, 4720.

TOC Figure

Encapsulation of Protonated Diamines in a Water-Soluble Chiral, Supramolecular Assembly Allows for Measurement of Nitrogen Inversion/Rotation (NIR)

Michael D. Pluth, Robert G. Bergman,* and Kenneth N. Raymond*